A DISSERTATION
FOR THE DEGREE OF DOCTOR OF PHILOSOPHY

Evaluation of the Anatomical Structures of the Iridocorneal Angle and Proximal Lacrimal Canaliculi Using Spectral Domain Optical Coherence Tomography

스펙트럼영역 빛간섭단층촬영기를 이용한 홍채각막각과 근위 누관의 해부학적 구조 평가

By

Jaeho Shim

MAJOR IN VETERINARY CLINICAL SCIENCES
DEPARTMENT OF VETERINARY MEDICINE
GRADUATE SCHOOL
SEOUL NATIONAL UNIVERSITY

August 2022

Evaluation of the Anatomical Structures of the Iridocorneal Angle and Proximal Lacrimal Canaliculi Using Spectral Domain Optical Coherence Tomography

by

Jaeho Shim

Supervised by
Professor Kangmoon Seo

Thesis
Submitted to the Faculty of the Graduate School
of Seoul National University
in Partial Fulfillment of the Requirements
for the Degree of Doctor of Philosophy
in Veterinary Medicine

April 2022

Major in Veterinary Clinical Sciences
Department of Veterinary Medicine
Graduate School
Seoul National University

June 2022

Evaluation of the Anatomical Structures of the Iridocorneal Angle and Proximal Lacrimal Canaliculi Using Spectral Domain Optical Coherence Tomography

스펙트럼영역 빛간섭단층촬영기 이용한 홍채각막각과 근위 누관의 해부학적 구조 평가

지도교수 서 강 문

이 논문을 수의학 박사 학위논문으로 제출함
2022 년 4 월

서울대학교 대학원
수의학과 임상수의학 전공
심 재 호

심재호의 박사학위논문을 인준함
2022 년 6 월

위 원 장 _____ (인)

부위원장 _____ (인)

위 원 _____ (인)

위 원 _____ (인)

위 원 _____ (인)

Evaluation of the Anatomical Structures of the Iridocorneal Angle and Proximal Lacrimal Canaliculi Using Spectral Domain Optical Coherence Tomography

Supervised by

Professor Kangmoon Seo

Jaeho Shim

Major in Veterinary Clinical Sciences

Department of Veterinary Medicine

Graduate School

Seoul National University

ABSTRACT

This study was to evaluate the microstructures of the eye including iridocorneal angle and lacrimal canaliculi (LC) by spectral-domain optical coherence tomography (SD-OCT).

In chapter 1, the feasibility of imaging the canine iridocorneal angle parameters in a clinical setting was investigated. A total of 47 eyes of dogs were scanned at the

temporal limbus using SD-OCT and UBM. Iridocorneal angle (ICA) and angle opening distance (AOD) were measured from the obtained images accordingly. The intra-observer and inter-observer reproducibility were evaluated using the intraclass correlation coefficient. To evaluate intra-observer reproducibility, measurements of the first and second grading from the first examiner were compared. To evaluate inter-observer reproducibility, measurements between the two examiners were compared. Bland-Altman plots were used to evaluate agreement between ICA and AOD for SD-OCT and ultrasound biomicroscopy (UBM). In the first grading, ICA and AOD for SD-OCT were 31.4 ± 6.4° and 641.4 ± 270.8 μm (mean ± SD), respectively. ICA and AOD for UBM were 32.0 ± 4.8° and 700.4 ± 238.8 μm (mean ± SD), respectively. For ICA and AOD measurements, intra-observer reproducibility was excellent for both devices, whereas inter-observer reproducibility was excellent for SD-OCT and good for UBM. The mean difference in ICA between SD-OCT and UBM was 0.6° with a limit of agreement (LoA) span of 18.9°. The mean difference in AOD between SD-OCT and UBM was 58.9 μm with a LoA span of 804.4 μm. SD-OCT is an effective non-contact imaging modality for the evaluation of canine iridocorneal angle parameters in a clinical setting. Reproducibility of measurements obtained is comparable or superior to UBM, but values obtained by SD-OCT and UBM for AOD are not interchangeable between devices.

In chapter 2, the feasibility of visualizing upper and lower proximal LC using SD-OCT was confirmed. Eight eyes of four normal Beagle dogs were included. To obtain an upper proximal LC image, the head was turned in the opposite direction to the eye being imaged, and the medial part of the upper eyelid was everted to expose

the LC. To obtain a lower LC image, the lower eyelid was everted just below the punctum. Using “angle mode”, the scan line was placed parallel on the long axis of the LC. The inlet LC width (LCW) was measured. Artificial tears (AT) were instilled, and LCW was compared before and after AT instillation. Additionally, the return time to the initial LCW inlet width was recorded. Before AT instillation, there was a significant difference between the mean upper and lower LCW (91.8 ± 3.2 and 110.1 ± 8.4 μm, respectively). After AT instillation, the mean upper and lower LCW were 236.9 ± 27.7 and 238.4 ± 30.4 μm, respectively. Significant differences in the LCW before and after AT instillation in both the upper and lower LCWs were observed. The mean return time of the upper and lower LCW to their initial widths after AT instillation was within 4 min. SD-OCT could be one option for providing high-resolution images of the upper and lower proximal LC. This method enables observation of LC changes after instillation of eyedrops in veterinary clinical practice.

In conclusion, SD-OCT would be an useful method for evaluating the ocular microstructures and the pathophysiological information of anterior segment of the eye and adnexa could be well confirmed.

Keywords: dog, glaucoma, iridocorneal angle, lacrimal canaliculi, SD-OCT, ultrasound biomicroscopy

Student number: 2018-27053

CONTENTS

GENERAL INTRODUCTION

Spectral domain optical coherence tomography (SD-OCT) is an interferometry technique that uses a low-coherence superluminescent light-emitting diode source. Commercially available SD-OCT have a short wavelength, allowing for faster scanning speed and improved axial and transverse resolution (Akil *et al.*, 2017b). It delivers non-invasive in vivo images that are directly associated to the histological appearance of the tissue (Hernandez-Merino *et al*., 2011). Previously, SD-OCT was widely used to image the transparent structures such as the cornea and the retina (Go *et al*., 2020; Wylęgała *et al*., 2009). In the recent years, it has been also used to monitoring ICA and imaging ocular adnexal tissue with the corneal adaptor module (cornea anterior module-low magnification, CAM-L) which helps to image the anterior segment of the eye (Allam and Ahmed, 2015; Jang *et al*., 2020; Singh *et al*., 2017; Sung *et al*., 2017; Timlin *et al*., 2016; Wawrzynski *et al*., 2014).

Glaucoma is a painful condition that is one of the most common causes of vision loss in mammals (Maggs, 2018). Primary angle closure glaucoma which impairs aqueous humor (AH) outflow is the most common form of canine glaucoma (Whiteman *et al*., 2002). Quantitative measurements of anterior ocular segment dimensions would be crucial because AH drainage is directly related to iridocorneal angle configuration (Puma *et al*., 2019).

In veterinary medicine, ultrasound biomicroscopy (UBM) has been utilized to assess the observation of tissues with near microscopic resolution (Katawa and Hasegawa, 2013; Park *et al*., 2015; Puma *et al*., 2019). However, UBM is a contact

method that could distort the image produced and necessitates topical anesthetic. SD-OCT, which has a greater imaging resolution than UBM, has recently been used in veterinary medicine to evaluate iridocorneal angle configuration (Almazan *et al*., 2013; Puma *et al*., 2019; Tsai *et al*., 2013). Compared to UBM, SD-OCT with improved image resolution increases detection of microscopic structures such as end of Descemet's membrane (Akil *et al*., 2017b). Since its use was limited to veterinary medicine to date, ICA was imaged by SD-OCT and measured parameters were compared between SD-OCT and UBM in dogs (Chapter 1).

Epiphora is an overflow of tears on the face and the commonly encountered clinical manifestation of diseases in the nasolacrimal drainage system in dogs (Park *et al*., 2016). The normal structure of lacrimal system plays an important role in lacrimal drainage and majority of epiphora is occurred due to deformities of the structure (Barnett, 1979; Park *et al*., 2016).

Considering the superficial location of the LC, UBM was used to visualize the structure (Gelatt *et al*., 2006; Quantz and Stiles, 2019; Tao *et al*., 2020). However, UBM could distort the actual lacrimal canaliculi structure and produced poor resolution images since the prove should be contacted to the examination site (Allam and Ahmed, 2015; Hurwitz *et al*., 2009; Sung *et al*., 2017). Alternatively, in human medicine, lacrimal scintigraphy, computed tomography dacryocystography, and magnetic resonance imaging have all been used to image the LC (Yan *et al*., 2020). However, these methods are not suitable for analyzing the proximal LC instead, and these procedures are more appropriate for analyzing the lacrimal duct (Tao *et al*., 2014; Yan *et al*., 2020).

Due to short wavelength of SD-OCT, the light penetration into opaque tissue would be limited (Timlin *et al*., 2017). However, the conjunctiva is naturally translucent, and LC is located superficial layer, SD-OCT light may penetrate the LC quite deeply, providing useful information for interpretating of lacrimal drainage system as well as its surrounding tissues (Chapter 2). Therefore, the feasibility of SD-OCT for imaging the anatomical characteristics of the proximal LC was evaluated in normal Beagle dogs.

The aim of this study was to evaluate the feasibility of imaging iridocorneal angle and proximal LC by using SD-OCT in dogs and it would provide the pathophysiological information of anterior segment of the eye and adnexa.

CHAPTER I

Comparison of Iridocorneal Angle Parameters Measured by Spectral Domain Optical Coherence Tomography and Ultrasound Biomicroscopy in Dogs

ABSTRACT

To compare the measurements of iridocorneal angle parameters between spectral domain optical coherence tomography (SD-OCT) and ultrasound biomicroscopy (UBM), a total of 47 eyes of dogs were scanned at the temporal limbus using SD-OCT and UBM were investigated. Iridocorneal angle (ICA) and angle opening distance (AOD) were measured from the obtained images accordingly. The intra-observer and inter-observer reproducibility were evaluated using the intraclass correlation coefficient. To evaluate intra-observer reproducibility, measurements of the first and second grading from the first examiner were compared. To evaluate inter-observer reproducibility, measurements between the two examiners were compared. Agreement between ICA and AOD for SD-OCT and UBM was evaluated using Bland–Altman plots. In the first grading, the mean ICA and AOD for SD-OCT were 31.4 ± 6.4° and 641.4 ± 270.8 μm, respectively. The mean ICA and AOD for UBM were 32.0 ± 4.8° and 700.4 ± 238.8 μm, respectively. For ICA and AOD measurements, intra-observer reproducibility was excellent for both devices, whereas inter-observer reproducibility was excellent for SD-OCT and good for UBM. The mean difference in ICA between SD-OCT and UBM was 0.6º with a limit of agreement (LoA) span of 18.9º. The mean difference in AOD between SD-OCT and UBM was 58.9 μm with a LoA span of 804.4 μm. SD-OCT is an effective non-contact imaging modality for the evaluation of canine iridocorneal angle parameters in a clinical setting. Reproducibility of measurements obtained is comparable or superior to UBM, but values obtained by SD-OCT and UBM for AOD are not interchangeable between devices.

INTRODUCTION

Glaucoma is often a painful disease and one of the leading causes of vision loss in mammalian species (Maggs, 2018). In glaucoma, the retinal ganglion cells and the nerve fiber layer undergo irreversible degeneration (Whiteman *et al*., 2002). In dogs, primary angle closure glaucoma (PACG), which impairs aqueous humor (AH) outflow, is the most common form of primary glaucoma (Whiteman *et al*., 2002). Iridocorneal angle configuration is related to the pathophysiology of AH drainage; therefore, objective, and reproducible measurements of iridocorneal angle parameters are crucial (Akil *et al.,* 2017b; Puma *et al*., 2019).

Ultrasound biomicroscopy (UBM) has been used to evaluate the anterior ocular segment in veterinary medicine (Park *et al*., 2015; Puma *et al*., 2019). This device provides cross-sectional images and biometric information of the anterior ocular segment, such as anterior chamber depth, ciliary cleft width, and length, and iridocorneal angle (Dulaurent *et al*., 2012; Park *et al*., 2015). However, the major drawback of UBM is the contact method, which potentially influences the image produced and requires topical anesthesia and a saline water bath.

Recently, spectral domain optical coherence tomography (SD-OCT), which provides a higher imaging resolution than UBM, has been introduced to study iridocorneal angle parameters in veterinary medicine (Almazan *et al*., 2013; Puma *et al*., 2019; Tsai *et al*., 2013). Although SD-OCT was primarily designed to image the fundus, it has been adapted to investigate anterior segment of the eye by attaching the corneal anterior module (Wylęgała *et al*., 2009). Improved image resolution of

SD-OCT enables detection of even a small structure, such as the end of Descemet's membrane (Akil *et al*., 2017a).

Both SD-OCT and UBM allow imaging of iridocorneal angle parameters. However, analysis of iridocorneal angle parameters obtained by SD-OCT have rarely been studied in dogs (Almazan *et al*., 2013). Therefore, the aim of this study was to compare iridocorneal angle parameters obtained from SD-OCT and UBM in dogs.

MATERIALS AND METHODS

1. Animals studied

A total of 47 eyes of 31 client-owned dogs, of which 13 were male and 18 were female, were examined in this study. The mean age ± standard deviation (SD) was 8.6 ± 4.3 years (range: 1 – 15 years). The mean intraocular pressure ± SD was 16.6 ± 4.3 mmHg (range: 8 – 25 mmHg). Twelve dog breeds were included in the study population: six Malteses, six miniature Poodles, four Shih Tzus, four Yorkshire terriers, two Chihuahuas, two Cocker Spaniels, two medium sized mixed breeds, two Pomeranians, and one each of the following breeds: Beagle, Bichon Frise, French Bulldog, and miniature Schnauzer. All dogs in this study presented at the Seoul National University Veterinary Medical Teaching Hospital with various ophthalmic diseases, including 7 normal eyes; 4 keratoconjunctivitis sicca; 13 eyelid diseases, including meibomian gland dysfunction, medial canthal trichiasis, and distichiasis; 15 incipient cataracts; 5 immature cataracts; 2 mature cataracts; and 4 hypermature cataract eyes. Based on the diagnosis of each dog, topical medications, including antibiotics, NSAIDs, cyclosporine, and artificial tears, were prescribed as treatments. However, dogs prescribed mydriatics or miotic medication were excluded from this study. Routine ophthalmic examinations, including neuro-ophthalmic examinations, slit-lamp biomicroscopy (SL-D7; Topcon Corp., Tokyo, Japan), and rebound tonometry (TONOVET-Plus®; Icare Finland Oy, Helsinki, Finland) were also performed.

The exclusion criteria were previous intraocular surgery, corneal ulcer, iridociliary mass, and severe corneal edema or pigmentation, which hampered the visualization of iridocorneal angle parameters by SD-OCT. The guidelines of the Institutional Animal Care and Use Committee of Seoul National University (SNU-200603-3) were followed for all procedures and animal care. The approval of each owner was acquired before the examination of the dogs was carried out.

2. Procedures

The anterior ocular segment was examined using SD-OCT (iVue® 100; Optovue Inc., Fremont, CA, USA) and UBM (MD-320W; MEDA Co., Ltd., Tianjin, China). Both SD-OCT and UBM examinations were performed in the same dark room to minimize the effect of illumination on the pupil by maintaining standardized light conditions. Spectral domain optical coherence tomography and UBM were used to measure iridocorneal angle parameters in a randomized order. A single examiner (JS) with experienced assistants obtained all the images using SD-OCT and UBM to reduce measurement error. Scanning was performed until images with clear anatomical landmarks, including the end of Descemet's membrane, iris, cornea, and sclera, were obtained. Low-quality images showing motion artifacts, pathological anatomies, and poorly defined landmarks due to shadows due to eyelids, lashes, and hair were excluded accordingly. The location of the scan was checked prior to all procedures so that the images were obtained

at the same point: 9 o'clock in the right eye and 3 o'clock in the left eye, respectively. No sedatives or anesthetics were used during image acquisition.

Iridocorneal angle parameters were scanned using a table-mounted SD-OCT, which operated at an 830 nm wavelength infrared light source and provided a scan speed of 26,000 axial scans per second, with a transverse resolution of 15 μm and an axial resolution of 5 μm, (Fernández-Vigo *et al*., 2015; Perera *et al*., 2012; Qin *et al*., 2013; Quek *et al*., 2012) and the corneal adaptor module (cornea anterior module-low magnification, CAM-L) was mounted to analyze the ICA parameters with dimensions of 6 × 2 mm. During the SD-OCT scan, the dogs were in a sitting position, and the head and neck were slightly tilted and turned in the opposite direction of the eye to be imaged in order to maximize exposure of the temporal ocular surface (Fig. 1). To obtain iridocorneal angle parameters, scans were performed at the center of the limbus in the temporal quadrants using the software with the angle scan mode.

Ultrasound biomicroscopy was performed with a hand-held 50-mHz transducer. With the dogs in the sitting position, one drop of topical anesthesia 0.5% proparacaine hydrochloride (Alcaine®; Alcon, Fort Worth, TX, USA) was administered accordingly. No additional coupling agent was used. The eye was examined using a probe placed perpendicular to the lateral limbus. The eyelid was held open manually to expose the lateral canthus. Care was taken to avoid distortion of the globe caused by the pressure application. Only images showing clear anatomical landmarks, including the corneoscleral limbus, iris, iridocorneal angle, and anterior lens capsule, were selected for analyses.

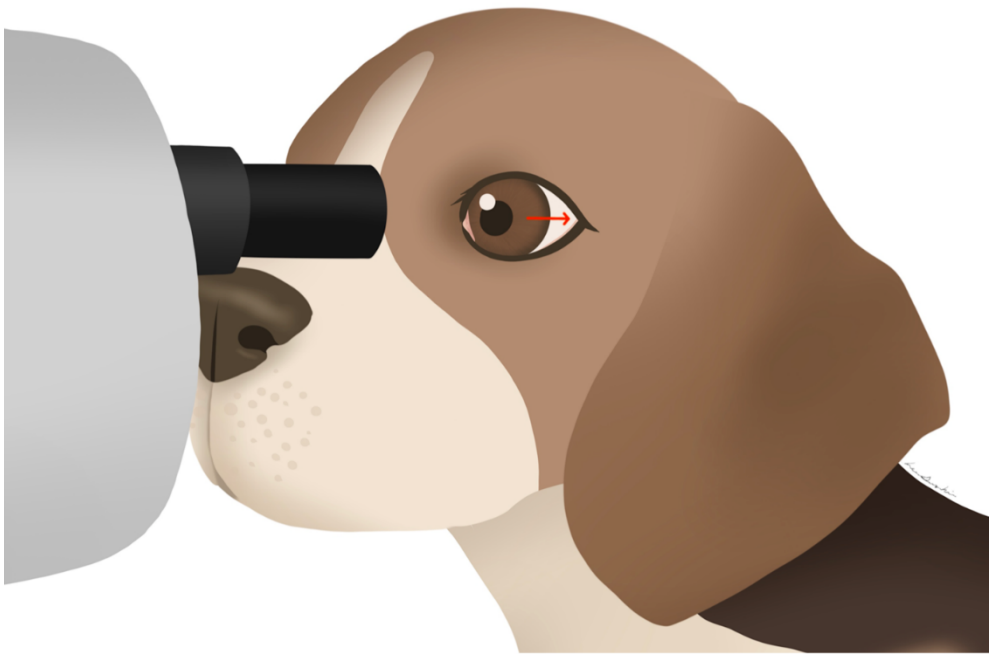

Fig. 1. Schematic diagram of imaging iridocorneal angle in the left eye by spectral domain optical coherence tomography. The dog was in the sitting position, and the head was slightly turned toward the opposite side to facilitate access to the eye being imaged to expose the temporal limbus, 9 o'clock for the right eye and 3 o'clock for the left eye.

3. Image analyses

The iridocorneal angle (ICA) and the angle opening distance (AOD) were measured as shown (Fig. 2). The ICA is formed by two lines, one line extending from the posterior limbus to the angle recess, and the other extending from the plane of the peripheral iris root (Dulaurent *et al*., 2012; Fernández-Vigo *et al*., 2016; Park *et al*., 2015). However, SD-OCT could not visualize the angle recess area; therefore, two virtual extension lines were elongated along the inner surface of the cornea and the peripheral iris, respectively. The angle was measured at the point at which the two lines met. AOD was defined as the distance (μm) along a perpendicular line from the end of Descemet's membrane to the iris surface. All SD-OCT and UBM images were exported to an external image processing software (ImageJ, NIH, Bethesda, MD) to measure ICA and AOD, and to eliminate the bias between the built-in software of the devices.

Based on the measurements, the intra-observer and inter-observer reproducibility of ICA and AOD were evaluated. For intra-observer reproducibility, measurements from the first and second grading by the first examiner were used for the analysis. The second grading was performed 1 week after the first grading. For inter-observer reproducibility, measurements from the first examiner (JS) and the second examiner (YJ) were compared. The second examiner is working in veterinary ophthalmology department of the same hospital. The second examiner graded the same image in the same manner as the first examiner. The grading interval and number of examiners were determined

according to the method of previous researches (Maram *et al*., 2015; Akil *et al.*, 2017a; Dastiridou *et al.*, 2015).

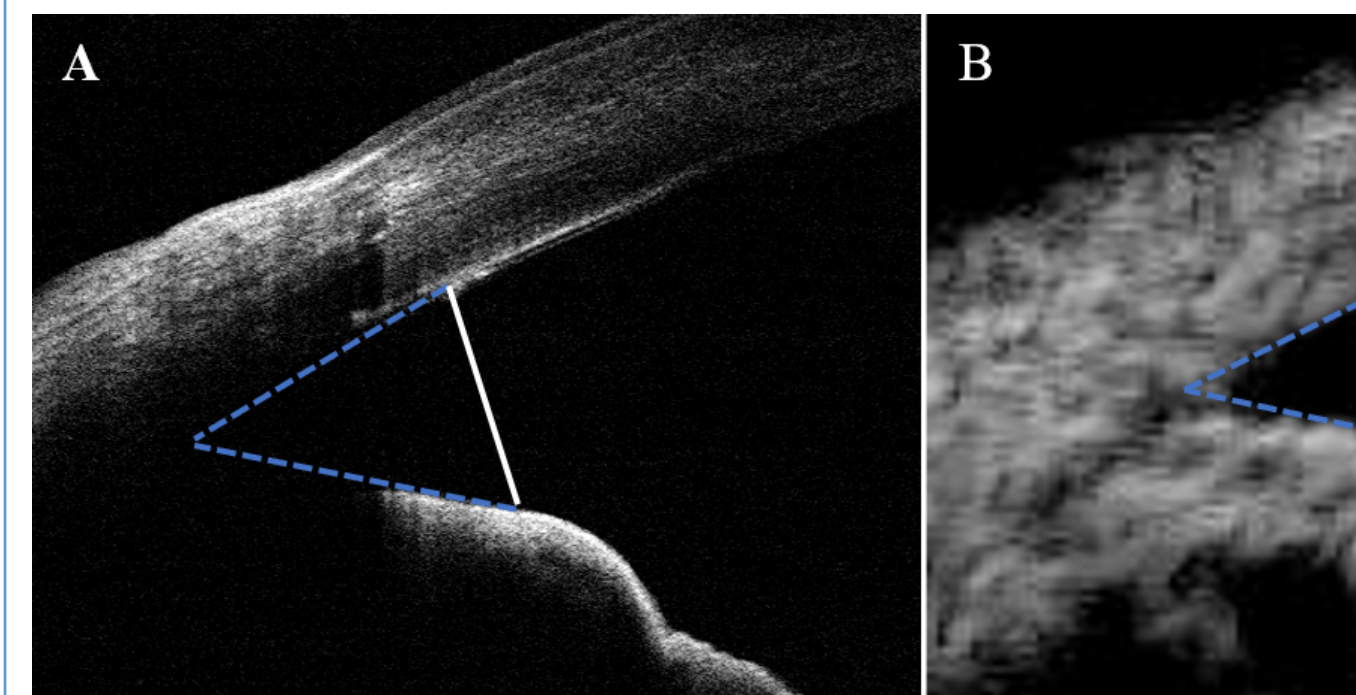

Fig. 2. Representative images of anterior chamber angle parameters measured using spectral domain optical co
and ultrasound biomicroscopy (UBM) for the right eye of the same dog. Iridocorneal angle is shown with a dashed
is shown with a solid line as viewed on SD-OCT (A) and UBM (B).

4. Statistical analyses

Measured iridocorneal angle parameters were expressed as mean ± SD. The intraclass correlation coefficient (ICC) of SD-OCT and UBM measurements was calculated as the degree of intra -and inter-observer reproducibility. The ICC indices were presented with 95% confidence intervals (CIs). The ICC indices between 0.60 and 0.74 indicated good clinical reliability and higher than 0.75 indicated excellent clinical reliability (Cicchetti, 1994).

Inter-device agreements between iridocorneal angle parameters obtained using SD-OCT and UBM were assessed using the Bland–Altman plot by evaluating the mean differences and limit of agreement (LoA). LoA was calculated as the mean difference ± 1.96 standard deviation.

Statistical analyses were performed using SPSS 25 (SPSS Inc., Chicago, IL, USA) and MedCalc 14.8.1.0 program (MedCalc Software, Mariakerke, Belgium).

RESULTS

1. Intra-observer reproducibility

All measurements by the first examiner were used to calculate the intra-observer reproducibility. Intra-observer reproducibility was tested by the second examiner and similar ICC values were identified. For SD-OCT, the mean ICA was 31.4 ± 6.4° (range: 20.8 – 52.3°) on the first grading and 31.0 ± 5.7° (range: 16.2 – 47.4°) on the second grading. The mean AOD for SD-OCT was 641.4 ± 270.8 µm (range: 141 – 1330 µm) on the first grading and 613.2 ± 266.3 µm (range: 138 – 1315 µm) on the second grading. Intra-observer reproducibility for SD-OCT for ICA and AOD was excellent.

For UBM, the mean ICA was 32.0 ± 4.8° (range: 21.6 – 42.9°) on the first grading and 31.8 ± 5.9° (range: 17.2 – 46.2°) on the second grading. The mean AOD for UBM was 700.4 ± 238.8 µm (range: 269 – 1312 µm) on the first grading and 730.7 ± 243.0 µm on the second grading (range: 193 – 1280 µm). The intra-observer reproducibility of all four measurements was excellent (Table 1).

Table 1. Intra-observer reproducibility with the iVue 100® SD-OCT and the UBM for the anterior char

		1st grading	2nd grading	Mean difference	ICC
SD-OCT (iVue 100®)	**ICA (º)**	31.4 ± 6.4†	31.0 ± 5.7	0.4	0.92
	AOD (µm)	641.4 ± 270.8	613.2 ± 266.3	28.3	0.97
UBM	**ICA (º)**	32.0 ± 4.8	31.8 ± 5.9	0.2	0.84
	AOD (µm)	700.4 ± 238.8	730.7 ± 243.0	30.4	0.89

† Mean ± standard deviation.
ICA, Iridocorneal angle; AOD, Angle opening distance; ICC, Intraclass correlation coefficient; CI, Cor

2. Inter-observer reproducibility

For SD-OCT, the mean ICA measured by the second examiner was 30.4 ± 6.6° (range: 15.4 – 47.5°) and the mean AOD measured by the second examiner was 588.0 ± 243.3 μm (range: 94 – 1037 μm). The inter-observer reproducibility for ICA and AOD measurements between the first and second examiners were excellent.

For UBM, the mean ICA by the second examiner was 31.4 ± 7.3° (range: 16.0 – 44.9°). The mean AOD measured by the second examiner was 899.4 ± 269.8 μm (range: 284 – 1724 μm). The mean difference between the first and second examiner measurements of AOD was 199.1 μm. The inter-observer reproducibility of ICA and AOD for UBM were good. UBM showed good ICC indices between examiners but was lower than that of SD-OCT (Table 2).

Table 2. Inter-observer reproducibility with the iVue 100® SD-OCT and the UBM for the anterior char

		1st examiner	2nd examiner	Mean difference	IC
SD-OCT (iVue 100®)	**ICA (º)**	31.4 ± 6.4†	30.4 ± 6.6	1.0	0.7
	AOD (µm)	641.4 ± 270.8	588.0 ± 243.3	53.5	0.9
UBM	**ICA (º)**	32.0 ± 4.8	31.4 ± 7.3	0.7	0.6
	AOD (µm)	700.4 ± 238.8	899.4 ± 269.8	199.1	0.6

† Mean ± standard deviation.
ICA, Iridocorneal angle; AOD, Angle opening distance; ICC, Intraclass correlation coefficient; CI, Cor

3. Agreement between SD-OCT and UBM

The mean ICA measurements were 31.4 ± 6.4° for SD-OCT and 32.0 ± 4.8° for UBM, based on the data from the first grading values with the first examiner. The mean difference in ICA values between SD-OCT and UBM was 0.6°, and the 95% LoA was -10.1 to 8.8° (Fig. 3A). The mean AOD measurements were 641.4 ± 270.8 μm for SD-OCT and 700.4 ± 238.8 μm for UBM. The mean difference between the two devices was 58.9 μm with a LoA of -461.1 to 343.3 μm (Fig. 3B).

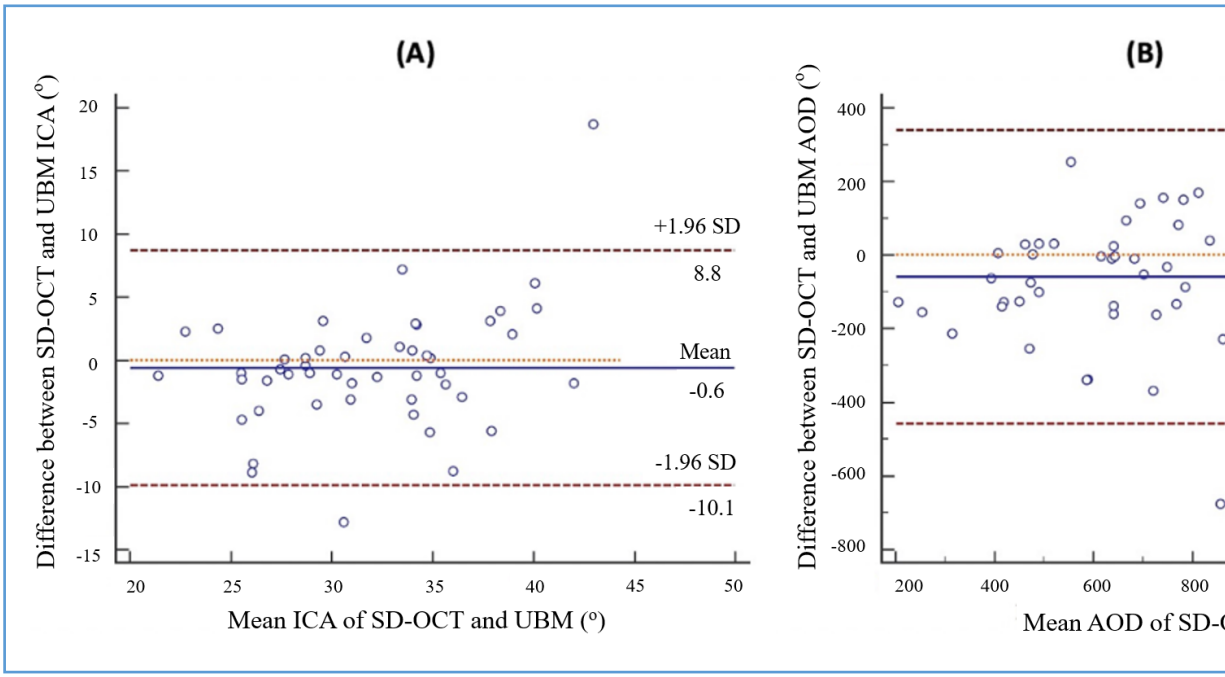

Fig. 3. Bland-Altman results for spectral domain optical coherence tomography (SD-OCT) and ultrasoun

Bland-Altman plots demonstrating the mean difference in and limit of agreement (LoA) of iridocor

opening distance (B) measurements between SD-OCT and UBM. The solid line indicates the mean d

lower LoA are represented by dashed lines on the side.

DISCUSSION

In this study, SD-OCT measurements of iridocorneal angle parameters showed excellent intra- and inter-observer reproducibility. These results suggested that within-and between-examiner bias showed a small variability in canines. The ICC indices for intra-observer reproducibility were excellent for UBM, but lower than those for SD-OCT. The inter-observer reproducibility of the UBM showed the lowest ICC, although it had good clinical reliability.

In the present study, all images made by SD-OCT and UBM were well visualized regardless of the angle width, and the procedure was well tolerated by the animals. In this study, variables that could affect the reproducibility between examiners, such as the scanning skill of an examiner and the environment during the scan, were eliminated by analyzing one identical image obtained by one examiner (Urbak *et al*., 1998). Additionally, when calculating intra-observer reproducibility, second grading was performed one week after the first acquisition to reduce the bias (Park *et al*., 2015). Previously, the intra-observer reproducibility indices for SD-OCT (Akil *et al*., 2017b; Dastiridou *et al*., 2015; Quek *et al*., 2012) and UBM (Park *et al*., 2015; Tello *et al*., 1994; Urbak *et al*., 1998) have been evaluated. Many iridocorneal angle parameters, including ICA, AOD, trabecular-iris space (TISA), and central corneal thickness, were assessed, and the intra-observer reproducibility was found to be reliable. The results of our study were similar to those of previous studies (Akil *et al*., 2017a; Dastiridou *et al*., 2015; Park *et al*., 2015; Quek *et al*., 2012; Tello *et al*.,

1994; Urbak *et al*., 1998). Our data showed excellent intra-observer reproducibility for ICA and AOD measurements for SD-OCT (ICC: 0.922 – 0.973) and UBM (ICC: 0.848 – 0.890). These results indicated the measurement error that could occur when one examiner repeatedly graded images that were clinically acceptable. However, if clear images were not selected at the time of scanning, the intra-observer reproducibility could decrease (Urbak *et al*., 1998). Therefore, to obtain reliable measurements, several scans should be performed until high quality images are acquired.

In addition to intra-observer reproducibility, the inter-observer reproducibility of the ICA parameters for SD-OCT was excellent in this study. Previous studies also reported excellent inter-observer reproducibility for AOD, and TISA measured using SD-OCT (Akil *et al*., 2017a; Akil *et al.,* 2017b; Dastiridou, *et al*., 2015). In contrast, the inter-observer reproducibility of UBM in our study was good. In previous UBM studies, failure to obtain reproducible ICA and AOD measurements between two examiners has been reported (Leung and Weinreb, 2011; Urbak *et al*., 1998). Other parameters, such as scleral thickness, iris thickness, and trabecular meshwork–iris distance were also examined, and significant differences between examiners were found (Tello *et al*., 1994; Urbak *et al*., 1998). The lower inter-observer reproducibility of UBM, compared with SD-OCT, might be due to the low resolution of UBM images included in this study. High-resolution SD-OCT could detect fine anatomical landmarks and indicate the reference points in detail (Leung *et al*., 2008; Tsai *et al*., 2013). Imaging clear anatomical landmarks is crucial because

quantification of the images depends on the individual recognition of the reference points, such as the end of Descemet's membrane, corneoscleral junction, and iris surface. Based on the results of this study, it might be best for a single observer to quantify the images because UBM measurements showed good inter-observer reproducibility and excellent intra-observer reproducibility. To improve the inter-observer reproducibility of UBM measurements, clinicians should use clear images with distinct reference points and well-defined descriptions of the parameters to be measured (Tello *et al*., 1994; Urbak *et al*., 1998). In addition, application of categorical data related to angle width instead of exact values could enhance the inter-observer reproducibility (Spaeth *et al*., 1997) but was not evaluated in the current study.

In this study, the mean AOD was 641.4 ± 270.8 μm for SD-OCT. The mean value was smaller than 1080 μm as reported in a previous study conducted in normal beagle dogs (Almazan *et al*., 2013). This might be due to the difference between the devices used, SD-OCT in the present study, and time domain anterior segment OCT, which has a longer wavelength, in the earlier study in beagles. Moreover, biological variation between breeds, ages and eye diseases could also contribute to these differences (Almazan *et al*., 2013).

According to a previous study, the agreement of AOD between the slit-lamp OCT and Visante® OCT was evaluated using Bland–Altman plots and its LoA span was 530 μm, suggesting a poor agreement (Leung and Weinreb, 2011). In other studies, comparing two different SD-OCT, a 520 μm span of LoA was observed, suggesting

moderate agreement (Akil *et al*., 2017a), and the 180 µm span was suggested to be in good agreement (Dastiridou *et al*., 2015). In this study, the LoA span of AOD between SD-OCT and UBM was 804.4 µm, which is greater than the LoA span of previous studies, indicating poor agreement. One previous study conducted in companion rabbits demonstrated a disagreement of AOD between SD-OCT and UBM and suggested that both the devices could not be used interchangeably, which is in accordance with our findings (Puma *et al*., 2019). The previous reports showed a good inter-device agreement with a LoA of 0.9 to 19.4° for ICA between SD-OCT and UBM (Ma *et al*., 2016). Our data showed that the LoA span of ICA between the devices was 18.9°, which was considered sufficiently narrow. Therefore, it was concluded that these two devices could be used interchangeably only for ICA measurements.

One major drawback of most commercially available SD-OCT devices, is their relatively short wavelength, and therefore, depth of tissue penetration, which limit visualization of angle recess area and ciliary cleft (CC) in dogs (Krema *et al*., 2013; Pan *et al*., 2016). Therefore, other ICA parameters such as CC area, and width and length of CC could not be evaluated by SD-OCT (Park *et al*., 2015). Furthermore, SD-OCT light is attenuated or absorbed by pigment within tissues (Park *et al*., 2015). As a result, it was difficult to evaluate iridocorneal angle parameters through the pigmented cornea and posterior part of the iris (Krema *et al*., 2013). However, the high resolution of the device enables the detection of small structures of the angle (Akil *et al*., 2017a). In this study, the end of the Descemet's membrane (Schwalbe's

line, SL) was used as an anatomical landmark to measure AOD and was found to have the highest reproducibility when compared to other landmarks. Therefore, further studies based on SL as an anatomical landmark to investigate new parameters for analyzing iridocorneal angle would be meaningful in canine patients.

There were several limitations to the present study. First, each scan might not have been performed at the exact same temporal location of the eye, even though we tried to focus on the 3 o'clock or 9 o'clock point of the eye. However, as the same examiner (JS) and experienced assistants performed all scans, the measurement errors could be minimized. In addition, according to a previous OCT study, (Pan *et al*., 2016) small changes in the scan location did not significantly alter iridocorneal angle parameters. Second, the pupil diameter was not measured in this study. Although the investigation was performed in the same dark room, ambient light intensity is not the sole determinant of pupil size. Therefore, the measurements could be varied. Third, the current study did not compare SD-OCT and UBM measurements with the reference standard, gonioscopy. Both SD-OCT and UBM are known to provide an objective measurement of iridocorneal angle parameters (Ma *et al*., 2016; Dastiridou *et al*., 2015; Tello *et al*., 1994). However, it was not possible to determine which imaging device provided similar results to the gonioscopy results in this study. Although a comparison was not performed in our study, previous studies showed a good correlation between gonioscopy results and SD-OCT measurements and between gonioscopy results and UBM measurements (Barkana *et al*., 2007; Dastiridou *et al*., 2015; Qin *et al*., 2013; Radhakrishnan *et al*., 2005).

Lastly, our study did not compare iridocorneal angle parameters in consideration of biological variables, such as age, breed, and eye disease. For example, cataract could change angle configuration, however, it might not affect reproducibility between two devices which was aim of our study. Therefore, future studies considering these variables might help predict changes in iridocorneal angle status in dogs.

CONCLUSION

SD-OCT is an excellent non-contact imaging device for evaluating ICA and AOD in a clinical setting. Reproducibility of measurements obtained is comparable or superior to UBM. However, values acquired by SD-OCT and UBM for AOD are not interchangeable between devices.

.

CHAPTER II

Evaluation of the Upper and Lower Lacrimal Canaliculus Using Spectral Domain Optical Coherence Tomography in Normal Beagle Dogs

ABSTRACT

To evaluate the changes in the upper and lower lacrimal canaliculi (LC) before and after artificial tears (AT) instillation using spectral domain optical coherence tomography (SD-OCT), eight eyes of four normal Beagle dogs were enrolled. To obtain an upper LC image, the head was turned contralateral to the eye being imaged and the medial part of the upper eyelid was everted to expose the LC. To obtain a lower LC image, the lower eyelid was everted just below the punctum. Using "angle mode", the scan line was placed parallel on the long axis of the LC. The inlet LC width (LCW) was measured. LCW was compared before and after AT instillation. Additionally, the return time to the initial LCW inlet width was recorded. Before AT instillation, there was a significant difference between the mean upper and lower LCW (91.8 ± 3.2 μm and 110.1 ± 8.4 μm, respectively). After AT instillation, the mean upper and lower LCW were 236.9 ± 27.7 μm and 238.4 ± 30.4 μm, respectively. Significant differences in the LCW before and after AT instillation in both the upper and lower LCWs were observed. The mean return time of the upper and lower LCW to their initial widths after AT instillation was within 4 min. Therefore, instill eye drops at 5 minutes interval would be reasonable. SD-OCT was an effective method to provide high resolution images of the upper and lower LC. This method enables observation of LC changes after instillation of eyedrops on a veterinary clinical practice.

INTRODUCTION

Epiphora is an overflow of tears on the face and the most common clinical manifestation of diseases in the nasolacrimal drainage system of dogs (Park *et al*., 2016). The majority of epiphora occurs due to deformities of the lacrimal drainage structure (Barnett, 1979; Park *et al*., 2016). The lacrimal canaliculi (LC) are part of the drainage system connected to the lacrimal punctum. Their normal size, location, and anatomy are the basis of tear dynamics (Fulmer *et al*., 1999; Tao *et al*., 2020).

Considering the superficial location of the LC, ultrasound biomicroscopy (UBM) is frequently used to visualize the structure (Gelatt *et al*., 2006; Quantz and Stiles 2019; Tao *et al*., 2020). However, the limitations of UBM are poor resolution images and contact with the examination site (Allam and Ahmed 2015; Hurwitz *et al*., 2009; Sung *et al*., 2017). Alternatively, the LC has been imaged using lacrimal scintigraphy, computed tomography dacryocystography, and magnetic resonance imaging in human medicine (Yan *et al*., 2020). Since these techniques are more appropriate for the examination of the lacrimal duct, it is difficult to evaluate the LC in detail (Tao *et al*., 2014; Yan *et al*., 2020).

Spectral domain optical coherence tomography (SD-OCT) has been used recently to image the LC in human medicine (Ishikawa *et al*., 2020; Singh *et al*., 2017; Sung *et al*., 2017; Tao *et al*., 2020; Timlin *et al*., 2016; Wawrzynski *et al*., 2014). It is a cross-sectional, high-resolution, and non-contact method using infrared light with a of wavelength 830 nm (Sung *et al*., 2017; Timlin *et al*., 2016; Wawrzynski *et al*.,

2014). The disadvantage of SD-OCT is that the device has a short wavelength limited to penetrating into the opaque tissue and only visualizing the superficial layer (Timlin *et al*., 2017). However, due to the translucent nature of the conjunctiva, a relatively deep penetration of SD-OCT light into the LC might be achieved and may provide useful information for understanding the lacrimal drainage system (Timlin *et al*., 2016).

This study aimed to evaluate the feasibility of SD-OCT for imaging the anatomical features of the proximal LC and to measure the width of the LC in normal Beagle dogs.

MATERIALS AND METHODS

1. Animals studied

Eight eyes of four normal Beagle dogs were included in this study. All dogs were male and aged approximately 1 year. The mean body weight was 10.7 ± 0.7 kg, and the mean Schirmer Tear Test value was 21.3 ± 1.51 mm/min. Routine ophthalmic examinations including neuro-ophthalmic examinations, slit-lamp biomicroscopy (SL-D7; Topcon Corp., Tokyo, Japan), Schirmer Tear Test® (MSD, Kenilworth, NJ, USA), rebound tonometry (TONOVET-Plus®; Finland Oy, Helsinki, Finland), and indirect ophthalmoscopy (Keeler Vantage Plus®; Keeler Ltd, Windsor, UK) were performed to exclude any ocular diseases. After ophthalmic examinations, the dogs with normal eyes were included in this study. Procedures and animal cares followed the guidelines of the Institutional Animal Care and Use Committee of Seoul National University (SNU-190930-5-2 and SNU-200729-1).

2. Imaging device

To image the LC, an SD-OCT scanner (iVue-100®; Optovue Inc., Fremont, CA, USA) was used. This device provides a scan speed of 26,000 axial scans per second at an infrared light-source wavelength of 830 nm (Fernández-Vigo *et al*.,

2015; Perera *et al*., 2012; Quek *et al*., 2012). The axial resolution was 5 μm, and the transverse resolution was 15 μm (Fernández-Vigo *et al*., 2015; Perera *et al*., 2012; Quek *et al*., 2012). The cornea anterior module-low magnification was mounted on SD-OCT to visualize the proximal LC.

3. Scanning procedures and image analyses

All dogs were sedated with medetomidine (Domitor®; Zoetis, Florham Park, NJ, USA) 0.002 mg/kg IV, titrated to a desired degree of sedation before the scanning procedure. The examination was performed in sternal recumbency. All the LC images were obtained by the same examiner with experienced assistants to reduce any measurement error. All images were converted to gray scale to improve image display (Tao *et al*., 2020). Both the upper and lower proximal LC of each eye of four dogs (eight eyes) were assessed. To obtain the upper LC image, the head was turned in the opposite direction of the eye to be imaged, and the nasal part of the upper eyelid was everted to achieve maximum upper LC exposure (Fig. 4A). To image the lower LC, the head was oriented in the forward direction with the face slightly tilted downward while in the sternal position. With the eye opened, the lower eyelid was gently everted directly below the lower lacrimal punctum. When everting the eyelid, care was taken to prevent the LC from being deformed due to excessive pulling (Fig. 4B). After everting the eyelid, the scan line was positioned on the long axis of the LC and images were obtained using the software with

"corneal angle mode" (Fig. 5). The scanning procedure was repeated to obtain the most open state of the LC, and the width of the inlet LC (LCW) was measured. LCW was measured at the endpoint of the LC epithelium (Fig. 6). All measurements were recorded using an adjustable built-in caliper in the SD-OCT machine. After scanning the upper and lower LC of each eye, three drops of artificial tears (AT) (Lacure®; Samil, Seoul, Republic of Korea) were administered. After AT instillation, the LC was observed by SD-OCT, and the return time to its initial width was recorded at 1 min intervals. The eyelid was manipulated only during scanning. After obtaining the LC image, the eyelids were left in a natural position between each LC scan-interval to minimize tear evaporation.

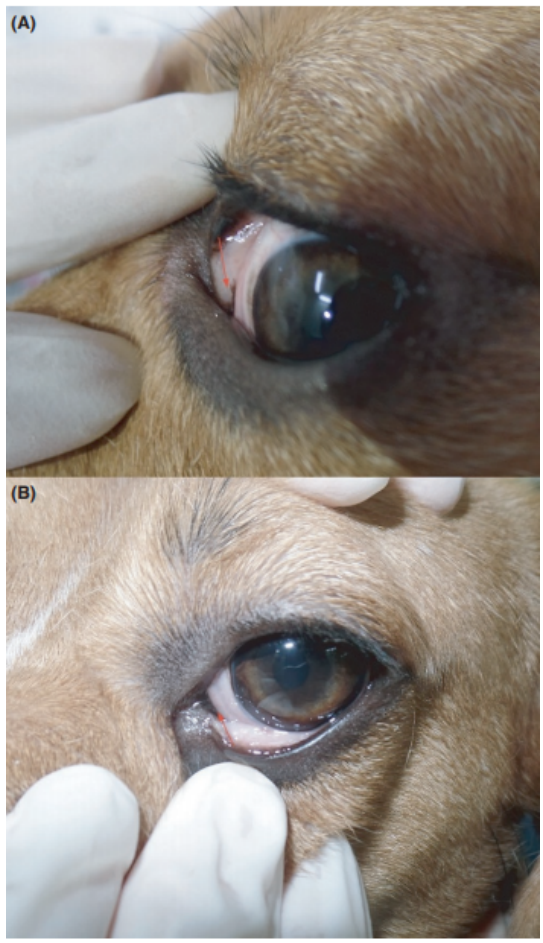

Fig. 4. Photographs of the manipulation of the eyelids for the imaging of the proximal lacrimal canaliculi (LC). (A) To obtain upper LC, the head is turned in the opposite direction of the eye to be imaged, and the nasal region of the upper eyelid is everted to optimize LC exposure. (B) To obtain lower LC, the lower eyelid is gently everted directly below the lower LC while the eye is opened. The scan line is placed parallel to the long axis of the LC (red arrow).

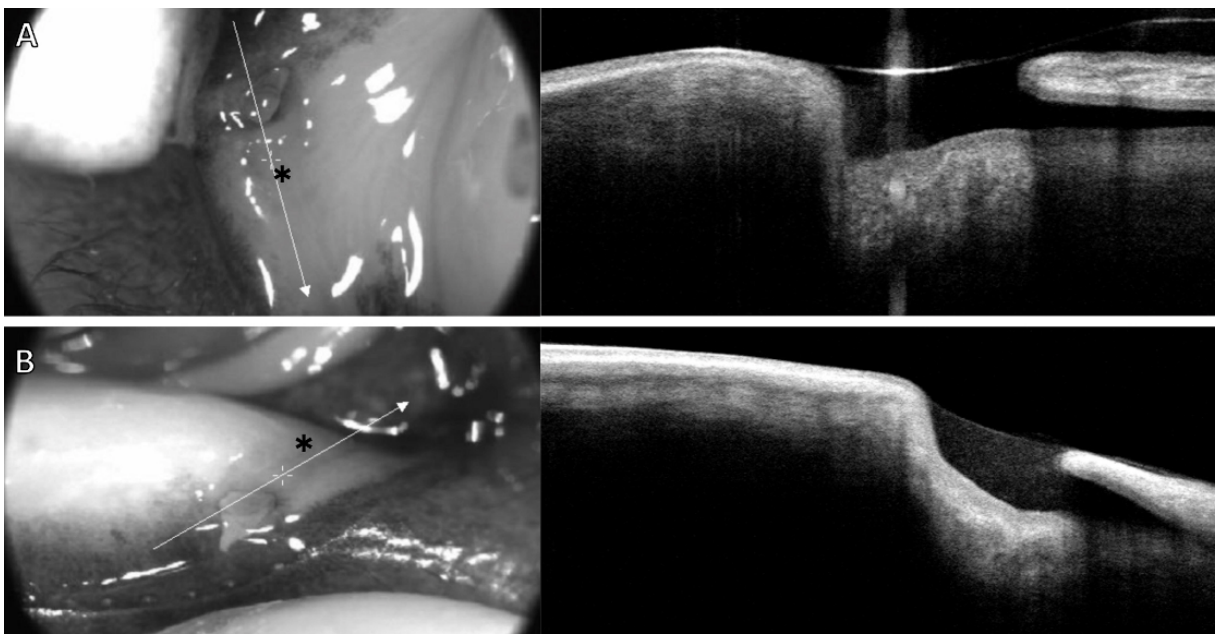

Fig. 5. Infrared (left) and optical coherence tomography (right) images. The scan line (*) is positione
upper and lower lacrimal canaliculi (LC). The scanning procedure is repeated to obtain the widest ope
(B) lower LC.

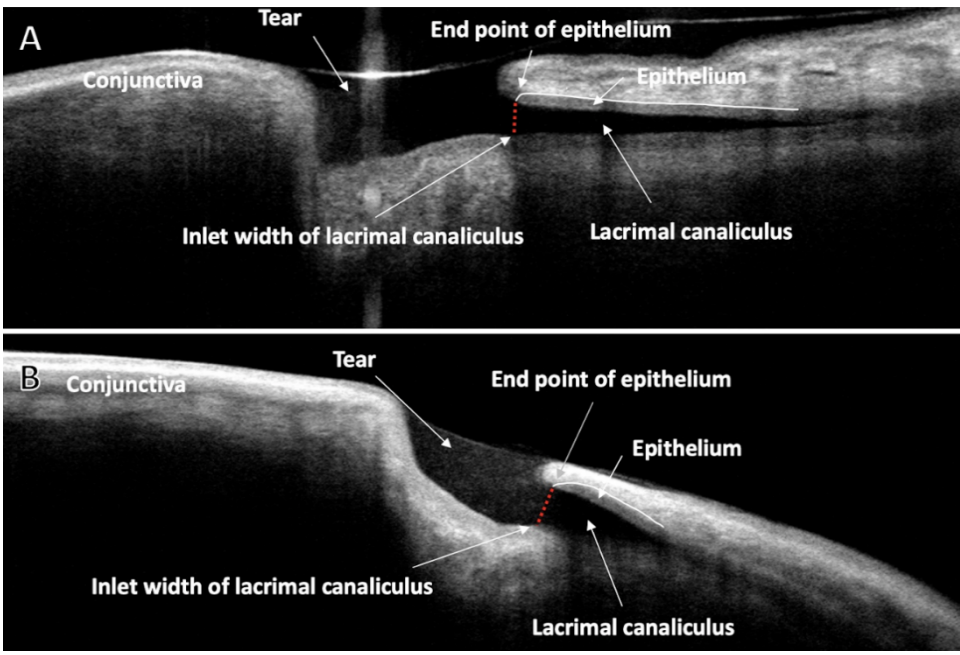

Fig. 6. Measurements of the inlet width of the (A) upper and (B) lower lacrimal canaliculus (LCW lacrimal canaliculi can be identified, including the canaliculus epithelium, tear, and conjunctiva.

4. Statistical analyses

Measured values are expressed as the mean ± standard deviation. Statistical analyses were performed using SPSS 25 (IBM Corp., Armonk, NY, USA). The Wilcoxon rank test was used to compare the widths of upper and lower LCs and also used to compare the values before and after AT instillation. In addition, the LCWs before and after the AT instillation were compared. The average return time to the initial width between the upper and lower LCW was compared. Statistical significance was defined as $P < 0.05$.

RESULTS

Before AT instillation, the mean widths of the upper and lower proximal LC were 91.8 ± 3.2 μm (range: 86−96 μm) and 110.1 ± 8.4 μm (range: 100−128 μm), respectively. The upper LCW was significantly narrower than the lower LCW (P = 0.012).

After AT instillation, both the upper and lower proximal LC were significantly expanded. The mean values of the upper and lower LCW were 235.5 ± 31.8 μm (range: 190−287 μm) and 238.4 ± 30.4 μm (range: 205−302 μm), respectively. Significant enlargement of the upper and lower LCW was noted between before and after AT instillation (P = 0.001). There was no significant difference between the upper and lower LCW after AT instillation (P = 1.000, Fig. 7).

Immediately after AT instillation, each upper and lower LC expanded and then returned to its initial width over time. The average return time of the upper and lower LC to their initial widths was 3.8 ± 0.7 min (range: 3−6 min) and 3.8 ± 0.9 min (range: 3−6 min), respectively. There was no significant difference between the return time for the upper and lower LCW (P = 1.000, Fig. 8).

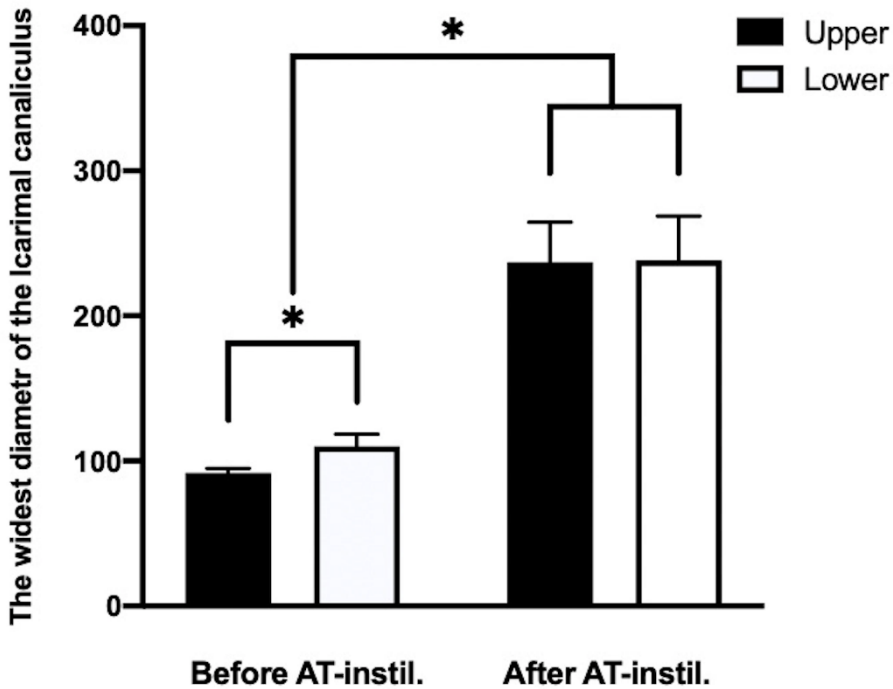

Fig. 7. Comparison of the inlet width of the upper and lower lacrimal canaliculus (LCW) before and after artificial tears (AT) instillation. Note the significant difference between the upper and lower LCW before AT instillation. However, LCW was significantly increased after AT instillation in both the upper and lower LCW and showed no significant difference between the two LCs.

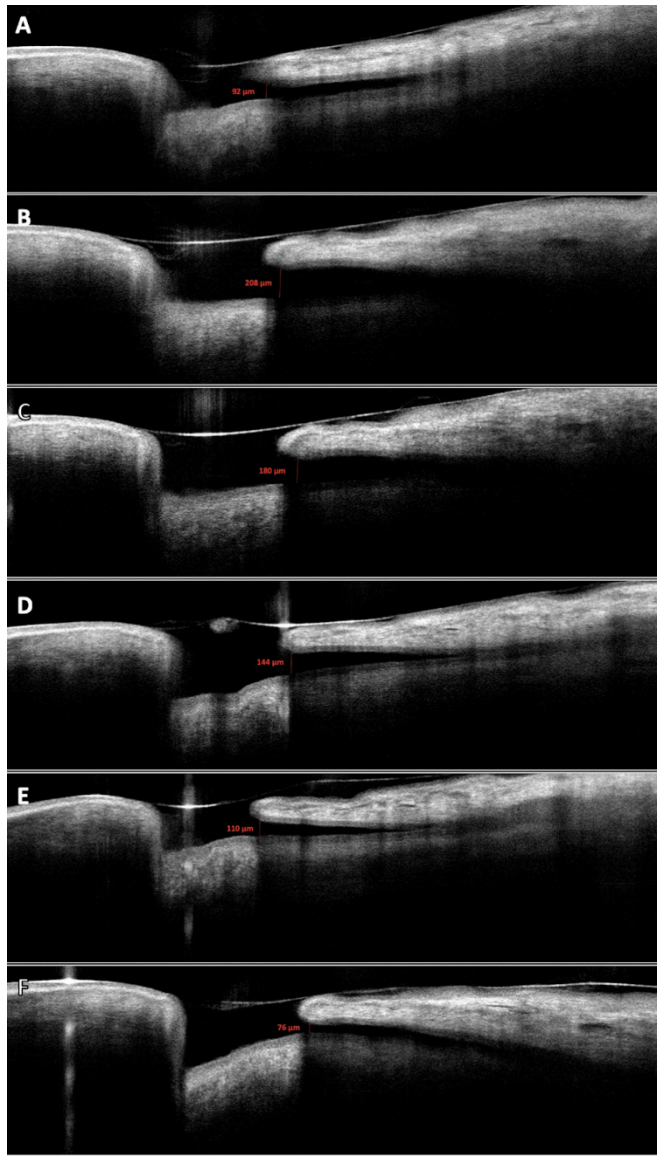

Fig. 8. Consecutive images after artificial tears (AT) instillation. (A) before AT instillation, (B) immediately after AT instillation, (C) 1 min, (D) 2 min, (E) 3 min, and (F) 4 min after AT instillation. Note the expansion of the LC immediately after AT instillation and the return to its initial state within 4 min.

DISCUSSION

This study provided high-resolution images and the first in vivo imaging of the proximal LC using SD-OCT in veterinary medicine. The high-resolution images enabled clear visualization of the proximal LC microstructures, such as the lumen, epithelium, and surrounding tissues. The scanning procedure was well tolerated, and the proximal LC were identifiable in all dogs.

In human studies, UBM has been used as an additional diagnostic tool to assess the LC (Hurwitz *et al*., 2009; Tao *et al*., 2014; Tao *et al*., 2020). However, viscoelastic materials should be filled within the LC to visualize the structures (Hurwitz *et al*., 2009; Singh *et al*., 2017). This procedure can distort the actual LC apparatus (Singh *et al*., 2017). In addition, the need for the UBM probe to contact the examination site and the low image resolution are major drawbacks of UBM (Allam and Ahmed, 2015; Jang *et al*., 2020; Sung *et al*., 2017; Timlin *et al*., 2016; Timlin *et al*., 2017). Dacryoendoscopy has also been used to evaluate the lacrimal excretory system in canine medicine (Tao *et al*., 2014; Yan *et al*., 2020). However, this is an invasive method requiring general anesthesia, and the LC may not be visualized in case of a congenital absence of the lacrimal punctum (Yan *et al*., 2020).

Spectral domain optical coherence tomography provides non-invasive in vivo images directly correlated to the histological tissue appearance (Hernandez-Merino *et al*., 2011). Its short wavelength cannot penetrate into opaque tissue. However, the conjunctiva is naturally translucent, allowing SD-OCT light to penetrate relatively

deep and demonstrating a high-resolution image of the LC without contact (Timlin *et al*., 2016). Furthermore, it can identify the LC features in the absence of the lacrimal puncta, as well as the relationship with its surrounding tissues (Yan *et al*., 2020). Predicting the presence or absence of LC is important for planning in patient with punctal occlusion (Timlin *et al.*, 2016).

In this study, the mean upper and lower LCW before AT instillation were narrower than those in a previous cadaveric study (Gelatt *et al.*, 1972). According to the previous study of a dolichocephalic dog, the LCW was 0.7-1.0 mm, which was larger than our measurement (Gelatt *et al*., 1972). This might be due to the difference between cadaveric and in vivo measurements (Singh *et al*., 2017). The LC is surrounded by muscle fibers in vivo and everting the eyelids could have altered the measurements of the LC in the current study, although the procedure was carefully performed (Ali *et al*., 2020; Singh *et al*., 2018).

In this study, the upper LCW was significantly narrower than the lower LCW before AT instillation. According to our results, the upper LC might have contributed less to tear drainage than the lower LC in normal conditions. Our results supported previous findings that the lower LC plays a major role in lacrimal drainage and that the blockage of the upper LC is usually asymptomatic (Bruce and Lynne, 2012; Park *et al*., 2016). However, after AT instillation, the upper and lower LCW were significantly enlarged, and there was no significant difference between the upper and lower LCW in this study. Expansion of lacrimal canaliculi might be due to the lacrimal pump mechanism with lids movement (Timlin *et al*., 2016). A study used a

drop test to evaluate the relative contribution of the upper and lower LC to lacrimal drainage capacity and showed that 40% of tears were drained through the upper LC (Murgatroyd *et al*., 2004). Other studies using fluorescein dye and dacryoscintigraphy suggested equal drainage capacity of each LC (Ögüt *et al*., 1993; White *et al*., 1989). Since the LCW was not directly translated to the lacrimal drainage capacity, the exact contribution to lacrimal drainage from each LC could not be determined in our study. However, since the upper LCW showed a significant expansion after AT instillation in this study, the upper LC was thought to have played an important role in tear drainage when the tear volume was increased, which is in line with previous studies (Murgatroyd *et al*., 2004; Ögüt *et al*., 1993; White *et al*., 1989).

The mean return time of LCW to its initial width was 3.8 ± 0.8 min. In this study, three drops of AT were instilled to achieve the widest image of the LC (Sahlin *et al*., 1998). The LC returned to its initial state within an average of 4 min in this study; therefore, it may be reasonable to instill eye drops at every 5 min (Maggs, 2018).

There were several limitations in this study. First, the factors which could affect lacrimal drainage, including blink rate, nature of the eye drops, and use of medetomidine as a sedative, were not considered (Fujimoto *et al*., 2018; Sahlin *et al*., 1998; Sanchez *et al*., 2006). An increased blink rate can significantly increase the lacrimal drainage capacity (Sahlin *et al*., 1998). Furthermore, medetomidine, a sedative used in this study, reduces tear production, which is in line with previous studies and may alter the tear drainage time in clinical practice. Therefore, further

studies that consider these factors would be required. Second, this study was conducted with a relatively small sample size. Further studies are required with large samples and with dogs experiencing lacrimal drainage system disorders to establish a normative database.

CONCLUSIONS

SD-OCT could visualized the upper and lower LC and provided quantified measurements of the LCW with high image resolution. In addition, investigating changes in the LC before and after AT instillation helped to better understand the tear dynamics as well as the anatomy of the lacrimal drainage system in dogs.

GENERAL CONCLUSIONS

Spectral domain optical coherence tomography (SD-OCT) is an excellent non-contact imaging device and provided high-quality images of iridocorneal angle configuration and proximal lacrimal canliculi (LC). In Chapter I of this study, reproducibility of SD-OCT was investigated and compared to that of ultrasound biomicroscopy (UBM). Inter-observer and intra-observer reproducibility of SD-OCT measurements were comparable or superior to UBM. However, values acquired by SD-OCT and UBM for angle opening distance (AOD) are not interchangeable between devices.

In Chapter II of the present study, SD-OCT allowed visualization of the upper and lower proximal LC effectively and provided quantified measurements of the lacrimal canaliculi width (LCW) with high image resolution. In addition, investigating changes of LCW before and after artificial tears (AT) instillation helped to better understand the tear dynamics as well as the anatomy of the proximal LC in dogs. Before AT instillation, the upper and lower LCW was narrower than those of after AT instillation. After AT instillation, the width of the upper and lower LC was widened and became comparable. The upper LCW showed a significant expansion after AT instillation, therefore, the upper LC was thought to play an important role in drainage when the tear volume was increased.

Through this study, SD-OCT could provide high-quality images of microstructures in anterior segment of the eye and its adnexa. Therefore, this device could be another option for imaging and understanding of iridocorneal angle configuration and the proximal lacrimal canaliculi.

REFERENCES

Akil H, Dastiridou A, Marion K, *et al*. Repeatability, reproducibility, agreement characteristics of 2 SD-OCT devices for anterior chamber angle measurements. *Can J Ophthalmol* 2017a;52:166-170.

Akil H, Marion K, Dastiridou A, *et al*. Identification of anterior chamber angle parameters with a portable SD-OCT device compared to a non-portable SD-OCT. *Int Ophthalmol* 2017b;37:31-37.

Ali MJ, Zetzsche M, Scholz M, *et al*. New insights into the lacrimal pump. *Ocul Surf* 2020;18:689-698.

Allam RS, Ahmed RA. Evaluation of the lower punctum parameters and morphology using spectral domain anterior segment optical coherence tomography. *J Ophthalmol* 2015;2015:1-7.

Almazan A, Tsai S, Miller PE, *et al*. Iridocorneal angle measurements in mammalian species: normative data by optical coherence tomography. *Vet Ophthalmol* 2013;16:163-166.

Barkana Y, Dorairaj SK, Gerber Y, *et al*. Agreement between gonioscopy and ultrasound biomicroscopy in detecting iridotrabecular apposition. *Arch Ophthalmol* 2007;125:1331-1335.

Barnett KC. Imperforate and micro-lachrymal puncta in the dog. *J Small Anim Pract* 1979;20:481-490.

Bruce HG, Lynne SS. Diseases and surgery of the canine nasolacrimal system, 2012. In: Gelatt KN, Gilger BC, Kern TJ, ed. Veterinary ophthalmology. 5th ed. Ames, IA: Wiley-Blackwell, 894–911.

Cicchetti DV. Guidelines, criteria, and rules of thumb for evaluating normed and standardized assessment instruments in psychology. *APA PsycNet* 1994;6:284-290.

Dastiridou A, Marion KM, Niemeyer M, *et al*. Agreement in quantitative anterior chamber angle metrics between RTVue and Cirrus spectral domain optical coherence tomography. *J Clin Exp Ophthalmol* 2015;6:1-7.

Dulaurent T, Goulle F, Dulaurent A, *et al*. Effect of mydriasis induced by topical instillations of 0.5% tropicamide on the anterior segment in normotensive dogs using ultrasound biomicroscopy. *Vet Ophthalmol* 2012;15:8-13.

Fernández-Vigo JI, Garcia-Feijoo J, Martinez-de-la-Casa JM, *et al*. Morphometry of the trabecular meshwork in vivo in a healthy population using fourier-domain optical coherence tomography. *Invest Ophthalmol Vis Sci* 2015;56:1782-1788.

Fernández-Vigo JI, Garcia-Feijoo J, Martínez-de-la-Casa JM, *et al*. Fourier domain optical coherence tomography to assess the iridocorneal angle and correlation study in a large Caucasian population. *BMC Ophthalmol* 2016;16:42.

Fujimoto M, Uji A, Ogino K, *et al*. Lacrimal canaliculus imaging using optical coherence tomography dacryography. *Sci Rep* 2018;8:1-8.

Fulmer NL, Neal JG, Bussard GM, *et al*. Lacrimal canaliculitis. *Am J Emerg Med* 1999;17:385–386.

Gelatt KN, Cure TH, Guffy MM, *et al*. Dacryocystorhinography in the dog and cat. *J Small Anim Pract* 1972;13:381-397.

Gelatt KN, MacKay EO, Widenhouse C, *et al*. Effect of lacrimal punctal occlusion on tear production and tear fluorescein dilution in normal dogs. *Vet Ophthalmol* 2006;9:23-27.

Go SM, Kang SM, Kwon J, *et al.* Optical coherence tomography of the Tokay gecko (*Gekko gecko*) eye. *Vet Ophthalmol* 2020;23:863-871.

Hernandez-Merino E, Kecova H, Jacobson SJ, *et al*. Spectral domain optical coherence tomography (SD-OCT) assessment of the healthy female canine retina and optic nerve. *Vet Ophthalmol* 2011;14:400-405.

Hurwitz JJ, Pavlin CJ, Hassan A. Proximal canalicular imaging utilizing ultrasound biomicroscopy A: normal canaliculi. *Orbit* 2009;17:27-30.

Ishikawa E, Sabundayo MS, Kono S, *et al*. Patency of the lacrimal drainage system in patients with a peripunctal tumour. *Orbit* 2020;39:102-106.

Jang JK, Lee SM, Lew H. A histopathological study of lacrimal puncta in patients with primary punctal stenosis. *Graefes Arch Clin Exp Ophthalmol* 2020;258:201-207.

Katawa M, Hasegawa T. Evaluation of the distance between Schwalbe's line and the anterior lens capsule as a parameter for the correction of ultrasound

biomicroscopic values of the canine iridocorneal angle. *Vet Ophthalmol* 2013;16:169-174.

Krema H, Santiago RA, Gonzalez JE, *et al*. Spectral-domain optical coherence tomography versus ultrasound biomicroscopy for imaging of nonpigmented iris tumors. *Am J Ophthalmol* 2013;156:806–812.

Leung CKS, Li H, Weinreb RN, *et al*. Anterior chamber angle measurement with anterior segment optical coherence tomography: a comparison between slit lamp OCT and visante OCT. *Invest Ophthalmol Vis Sci* 2008;49:3469-3474.

Leung CKS, Weinreb RN. Anterior chamber angle imaging with optical coherence tomography. *Eye* 2011;25:261-267.

Ma XY, Zhu D, Zou J, *et al*. Comparison of ultrasound biomicroscopy and spectral-domain anterior segment optical coherence tomography in evaluation of anterior segment after laser peripheral iridotomy. *Int J Ophthalmol* 2016;9:417-423.

Maggs DJ. Ophthalmic medications and therapeutic, 2018. In: Maggs DJ, Miller PE, Ofri R. ed. Slatter's fundamentals of veterinary ophthalmology. 6th ed. St. Louis, MO: Elsevier Inc, 51–88.

Maram J, Pan X, Francis B, *et al*. Reproducibility of angle metrics using the time-domain anterior segment optical coherence tomography: intra-observer and inter-observer variability. *Curr Eye Res* 2015;40:496-500.

Murgatroyd H, Craig JP, Sloan B. Determination of relative contribution of the superior and inferior canaliculi to the lacrimal drainage system in health using the drop test. *Clin Exp Ophthalmol* 2004;32:404-410.

Ögüt MS, Bavbek T, Kazokoglu H. Assessment of tear drainage by fluorescein dye disappearance test after experimental canalicular obstruction. *Acta Ophthalmol* 1993;71:69-72.

Pan X, Maram J, Marion K, *et al*. Effect of angle of incidence on anterior chamber angle metrics from optical coherence tomography. *J Glaucoma* 2016;25:e19-e23.

Park EJ, Kang SM, Park SW, *et al*. Congenital anomalies of lower lacrimal puncta and nasolacrimal duct atresia in a Labrador Retriever Dog. *Korean J Vet Res* 2016;33:228-230.

Park SW, Kang SM, Lee EJ, *et al*. Ultrasound biomicroscopic study of the effects of topical latanoprost on the anterior segment and ciliary body thickness in dogs. *Vet Ophthalmol* 2015;19:498-503.

Perera SA, Ho CL, Aung T, *et al*. Imaging of the iridocorneal angle with the RTVue spectral domain optical coherence tomography. *Invest Ophthalmol Vis Sci* 2012;53:1710-1713.

Puma MC, Freeman KS, Cleymaet AM, *et al*. Iridocorneal angle assessment of companion rabbits using gonioscopy, spectral-domain optical coherence tomography (Optovue iVue®), high-resolution ultrasound, and Pentacam® HR imaging. *Vet Ophthalmol* 2019;22:834-841.

Qin B, Francis BA, Li Y, *et al*. Anterior chamber angle measurements using Schwalbe's line with high resolution fourier-domain optical coherence tomography. *J Glaucoma* 2013;22:684-688.

Quantz K, Stiles J. Punctal stenosis in 6 dogs following the long-term use of topical neomycin-polymyxin B-dexamethasone. *Vet Ophthalmol* 2019;22:196-200.

Quek DT, Narayanaswamy AK, Tun TA, *et al*. Comparison of two spectral domain optical coherence tomography devices for angle-closure assessment. *Invest Ophthalmol Vis Sci* 2012;53:5131-5136.

Radhakrishnan S, Goldsmith J, Huang D, *et al*. Comparison of optical coherence tomography and ultrasound biomicroscopy for detection of narrow anterior chamber angles. *Arch Ophthalmol* 2005;123:1053-1059.

Sahlin S, Laurell CG, Chen E, *et al*. Lacrimal drainage capacity, age and blink rate. *Orbit* 1998;17:155-159.

Sanchez RF, Mellor D, Mould J. Effects of medetomidine and medetomidine-butorphanol combination on Schirmer tear test 1 readings in dogs. *Vet Ophthalmol* 2006;9:33-37.

Singh S, Ghosh A, Rath S. Imaging of proximal lacrimal system with time domain anterior segment optical coherence tomography in Asian Indian population. *Orbit* 2017;36:251-255.

Singh S, Rajput A, Mohamed A, *et al*. Spectral domain optical coherence tomography for measuring tear film meniscus height and its relationship with epiphora. *Indian J Ophthalmol* 2018;66:1592-1594.

Spaeth GL, Azuara-Blanco A, Araujo SV, *et al*. Intraobserver and interobserver agreement in evaluating the anterior chamber angle configuration by ultrasound biomicroscopy. *J Glaucoma* 1997;6:13-17.

Sung Y, Park JS, Lew H. Measurement of lacrimal punctum using spectralis domain anterior optical coherence tomography. *Acta Ophthalmol* 2017;95:e619-e624.

Tao H, Xu LP, Han C, *et al*. Diagnosis of lacrimal canalicular diseases using ultrasound biomicroscopy: a preliminary study. *Int J Ophthalmol* 2014;7:659-662.

Tao H, Wang YS, Wang F, *et al*. Diagnosis of lacrimal punctum lesions using optical coherence tomography: a preliminary study. *Int J Ophthalmol* 2020;13:902-906.

Tello C, Liebmann J, Potash SD, *et al*. Measurement of ultrasound biomicroscopy images: intraobserver and interobserver reliability. *Invest Ophthalmol Vis Sci* 1994;35:3549-3552.

Timlin HM, Keane PA, Day AC, *et al*. Characterizing the lacrimal punctal region using anterior segment optical coherence tomography. *Acta Ophthalmol* 2016;94:154-159.

Timlin HM, Keane PA, Rose GE, *et al*. The application of infrared imaging and optical coherence tomography of the lacrimal punctum in patients undergoing punctoplasty for epiphora. *Ophthalmol* 2017;124:910-917.

Tsai S, Almazan A, Lee SS, *et al*. The effect of topical latanoprost on anterior segment anatomic relationships in normal dogs. *Vet Ophthalmol* 2013;16:370-376.

Urbak SF, Pedersen JK, Thorsen TT. Ultrasound biomicroscopy. II. Intraobserver and interobserver reproducibility of measurements. *Acta Ophthalmol Scand* 1998;76:546-549.

Wawrzynski JR, Smith J, Sharma A, *et al*. Optical coherence tomography imaging of the proximal lacrimal system. *Orbit* 2014;33:428-432.

White WL, Glover AT, Buckner AB, *et al*. Relative canalicular tear flow as assessed by dacryoscintigraphy. *Ophthalmol* 1989; 96:167–169.

Whiteman AL, Klauss G, Miller PE, *et al*. Morphologic features of degeneration and cell death in the neurosensory retina in dogs with primary angle-closure glaucoma. *Am J Vet Res* 2002;63:257-261.

Wylęgała E, Teper S, Nowińska AK, *et al*. Anterior segment imaging: Fourier-domain optical coherence tomography versus time-domain optical coherence tomography. *J Cataract Refract Surg* 2009;35:1410-1414.

Yan X, Xiang N, Hu W, *et al*. Characteristics of lacrimal passage diseases by 80-MHz ultrasound biomicroscopy: an observational study. *Graefe Arch Clin Exp Ophthalmol* 2020;258:403-410.

국 문 초 록

스펙트럼영역 빛간섭단층촬영기를 이용한 홍채각막각과 근위 누관의 해부학적 구조에 관한 평가

지도교수 서 강 문

심 재 호

서울대학교 대학원

수의학과

임상수의학 전공

본 연구에서는 눈의 전안부 구조 및 부속기를 조사하기 위해 빛간섭단층촬영기를 이용하여 홍채각막각과 눈물관을 포함한 눈의 미세구조를 평가하였다.

제 1 장에서는 임상 환경에서 홍채각막각 척도의 영상화 가능성을 조사하였다. 빛간섭단층촬영기 및 초음파 생체 현미경을 이용하여 개의 외측 안륜부에서 총 47 개의 눈을 검사하였다. 이에 따라 획득한 영상으로부터 홍채각막각(ICA)과 각개방거리(AOD)를 측정하였다. 관찰자 내 및 관찰자 간 재현성은 급내 상관 계수를 사용하여 평가하였다. 관찰자 내 재현성을 평가하기 위해 첫 번째 검사자의 첫 번째 및 두 번째 등급 측정값을 비교하였다. 관찰자 간 재현성을 평가하기 위해 두 검사자 간의 측정값을 비교하였다. 빛간섭단층촬영기 및 초음파 생체현미경에 대한 홍채각막각과 각개방거리 간의 일치는 Bland-Altman plot 을 사용하여 평가하였다. 첫 번째 평가에서 빛간섭단층촬영기에 대한 평균 홍채각막각 및 각개방거리는 각각 31.4 ± 6.4°및 641.4 ± 270.8 μm 였다. 초음파 생체현미경에 대한 평균 홍채각막각과 각개방거리는 각각 32.0 ± 4.8°와 700.4 ± 238.8 μm 였다. 홍채각막각 및 각개방거리 측정의 경우 두 기기 모두에서 관찰자 내 재현성이 우수한 반면 빛간섭단층촬영기에서는 관찰자 간 재현성이 우수하고 초음파 생체현미경에서는 양호했다. 빛간섭단층촬영기와 초음파 생체현미경 사이의 홍채각막각의 평균 차이는 0.6° 였으며, 일치 한계 범위는 18.9° 였다. 빛간섭단층촬영기와 초음파 생체현미경 사이의 각개방거리 평균 차이는 58.9 μm 였고 일치 한계는 804.4 μm 였다. 빛간섭단층촬영기는 임상 환경에서 홍채각막각

척도의 평가를 위한 효과적인 비접촉 영상 기법이다. 빛간섭단층촬영기로 얻은 측정 값의 재현성은 초음파 생체현미경과 비슷하거나 우수하지만, 각개방거리 값은 초음파 생체 현미경으로 측정한 값과 교차하여 사용할 수 없었다.

제 2 장에서는 빛간섭단층촬영기를 사용하여 상부 및 하부 근위 누관 영상화 가능성을 확인하였다. 정상 비글견 4 마리에서 8 개의 눈이 실험에 포함되었다. 상안검의 누관 근위부 영상을 얻기 위해 영상화하고자 하는 눈의 내측 방향으로 머리를 돌리고 상안검의 내측 부분을 외번하여 상누관 근위부를 노출시켰다. 하누관 근위부 이미지를 얻기 위해 누점 바로 아래에서 하안검을 외번하였다. "각도 모드"를 사용하여 촬영 기준선을 누관의 장축에 평행하게 배치하여 누관 근위부 입구 폭을 측정했다. 인공눈물을 점안하고, 인공눈물 점안 전과 후의 누관 근위부 폭을 비교하였다. 또한 누관이 확장된 후 초기 누관 근위부 입구 폭으로 되돌아오는 시간인 회귀 시간을 기록했다. 인공눈물 점적 전에는 상누관과 하누관 근위부 폭 사이에 유의한 차이가 있었다(각각 91.8 ± 3.2 및 110.1 ± 8.4 μm). 인공눈물 점적 후 평균 상누관 및 하누관 근위부 폭는 각각 236.9 ± 27.7 및 238.4 ± 30.4 μm 였다. 상누관 및 하누관 근위부 폭은 인공눈물 점적 전후의 누관 근위부 폭과 유의한 차이가 관찰되었다. 인공눈물 점적 후 상부 및 하부 누관 근위부 폭의 초기 너비로의 평균 회귀 시간은 4 분 이내였다.

빛간섭단층촬영기는 상부 및 하부 누관 근위부를 고해상도 이미지로 촬영 할 수 있는 효과적인 방법이었다. 이 방법을 사용하여 수의학 임상에서 점안액 점안 후 누관 근위부 변화를 관찰할 수 있었다.

본 연구 결과, 빛간섭단층촬영기는 안구 미세구조를 평가하는데 유용한 방법으로 판단되며 이를 통해 안구의 전안부 및 부속기의 미세구조의 병태생리학적 정보를 잘 확인할 수 있을 것으로 사료된다.

주요어: 개, 빛간섭단층촬영기, 녹내장, 누관, 우각, 초음파 생체현미경

학번: 2018-27053